Doped Ceria Hot Paper

DOI: 10.1002/anie.201404618

Defect Chemistry of Singly and Doubly Doped Ceria: Correlation between Ion Transport and Energetics**

Salih Buyukkilic, Sangtae Kim, and Alexandra Navrotsky**

Abstract: *Earlier studies have shown a strong correlation between the enthalpy of formation, $\Delta H_{f,ox}$, and the ionic conductivity, σ_i, near room temperature in doped ceria systems, which are promising solid electrolytes for intermediate-temperature solid oxide fuel cells (IT-SOFCs). The present work demonstrates that this correlation holds at the operating temperature of IT-SOFCs, 600–700 °C. Solid solutions of $Ce_{1-x}Nd_xO_{2-0.5x}$, $Ce_{1-x}Sm_xO_{2-0.5x}$, and $Ce_{1-x}Sm_{0.5x}Nd_{0.5x}O_{2-0.5x}$ are studied. The $\Delta H_{f,ox}$ at 702 °C is determined by considering the excess heat content between 25 and 702 °C combined with the value of $\Delta H_{f,ox}$ at 25 °C. Both σ_i and $\Delta H_{f,ox}$ show maxima at $x = 0.15$ and 0.20 for the singly and doubly doped ceria, respectively, suggesting that the number of mobile oxygen vacancies in these solid solutions reaches a maximum near those compositions. An increase in temperature results in a shift of the maximum in both $\Delta H_{f,ox}$ and σ_i towards higher concentrations. This shift results from a gradual increase in dissociation of the defect associates.*

Rare earth (RE) doped ceria is one of the most extensively studied solid electrolytes for intermediate-temperature solid oxide fuel cells (IT-SOFCs)[1] because of superior oxygen ion conductivity, σ_i, at relatively low temperatures (500–700 °C).[2] As relatively abundant and accessible rare-earth elements,[3] cerium, neodymium, and samarium could yet emerge as the basis for financially feasible electrolytes for IT-SOFC applications. Oxygen ion conduction in such solid solutions involves thermally activated hopping of O^{2-} via oxygen vacancies (V_O^{2+}) in the crystal lattice at a rate that depends primarily on the concentration and mobility of the V_O^{2+} sites. While the stoichiometric number of V_O^{2+} sites in trivalent doped ceria increases linearly with dopant concentration, c_d, because of charge compensation, the mobility of the V_O^{2+} is governed by a complex potential energy landscape (PEL), which varies with temperature as well as with the c_d value that is provided by the host lattice.[4] Therefore, the σ_i of RE-doped ceria does not increase linearly with the number of V_O^{2+} sites introduced by doping, but shows common characteristics that can be summarized as follows: 1) σ_i presents a maximum with increasing c_d; 2) the activation energy, E_a, of σ_i increases with c_d; and 3) E_a at sufficiently high temperatures is lower than that at sufficiently low temperatures, and the critical temperature near which the transition in E_a occurs increases with c_d. These characteristics are generally indicative of substantial interactions between the charged defects, which become more pronounced at higher c_d and lower temperature, leading to the formation of various types of defect "associates", which induce substantial modification of the PEL. The E_a then increases accordingly, and σ_i decreases.[5] Therefore, the E_a has been considered as a primary parameter that measures the defect interactions in O^{2-}-conducting solid electrolytes.

It has recently been demonstrated that information about the defect interactions in oxide solid solutions can also be obtained by measuring their formation enthalpy from the oxides, $\Delta H_{f,ox}$, as a function of c_d.[6] For instance, the endothermic $\Delta H_{f,ox}$ of CeO_2–$REO_{1.5}$[7] at room temperature shows a maximum with increasing c_d.[7] The initial increase in $\Delta H_{f,ox}$ to more endothermic values with increasing c_d is attributed to lattice strain and local site distortion caused by the size mismatch between the host and dopant cations, whereas the defect interactions that occur at higher c_d stabilize the solid solution, leading to the decrease to less endothermic $\Delta H_{f,ox}$ values. These results imply that a unique correlation may exist between macroscopic V_O^{2+} dynamics in the oxide solid solution and the thermodynamic parameters of the solid-solution formation. Indeed, Avila-Paredes et al.[8] have shown that a pronounced maximum in $\Delta H_{f,ox}$ for lanthanum- and gadolinium-doped CeO_2 determined at room temperature appears at or near the c_d associated with maximum σ_i (namely the critical dopant concentration, c_d*) measured at relatively low temperatures. A similar correlation has also been observed in RE-doped thoria systems.[9]

Although these results strongly suggest a correlation between σ_i and the energetics near room temperature,[8–10] the existence of a similar correlation at higher temperatures has not yet been confirmed. This information would be more relevant to the application of such systems. Herein, we report a correlation between the σ_i and $\Delta H_{f,ox}$ values of ceria doped with Nd^{3+} ($Ce_{1-x}Nd_xO_{2-0.5x}$, xNDC), Sm^{3+} ($Ce_{1-x}Sm_xO_{2-0.5x}$, xSDC), and co-doped with both cations ($Ce_{1-x}Sm_{0.5x}Nd_{0.5x}O_{2-0.5x}$, xSNDC) near 700 °C, which is representative of the IT-SOFC operating temperature. The $\Delta H_{f,ox}$ values at 702 °C, $\Delta H_{f,ox}{}^{702\,°C}$, were determined as a function of

[*] Dr. S. Buyukkilic, Prof. S. Kim, Prof. A. Navrotsky
Department of Chemical Engineering and Materials Science
University of California
Davis, CA 95616 (USA)
E-mail: chmkim@ucdavis.edu
anavrotsky@ucdavis.edu
Dr. S. Buyukkilic, Prof. A. Navrotsky
Peter A. Rock Thermochemistry Laboratory and NEAT ORU
University of California
Davis, CA 95616 (USA)

[**] We thank Tien Tran Roehling for the SPS experiments and Seong Kim for technical support with the impedance measurements. This work was supported by the U.S. Department of Energy, Office of Basic Energy Sciences (03ER46053).

Supporting information for this article is available on the WWW under http://dx.doi.org/10.1002/anie.201404618.

c_d by measuring the excess heat content between 25 and 702 °C, $\Delta_{25\,^\circ C}^{702\,^\circ C}H_{xs}$, by transposed temperature drop calorimetry combined with $\Delta H_{f,ox}$ at room temperature, which was previously reported.[10] As demonstrated below, the correlation is maintained at temperatures as high as 700 °C such that the information about the c_d* values under IT-SOFC operating conditions can be obtained from the $\Delta H_{f,ox}$ values of the solid solutions and vice versa. The calorimetric data can further be used to directly obtain defect clustering energetics at both high and low temperatures.

Samples were synthesized by co-precipitation methods.[10] Powder X-ray diffraction (XRD) patterns (see the Supporting Information) of *x*NDC, *x*SDC, and *x*SNDC solid solutions with $x = 0.05$–0.30 at room temperature confirmed the formation of single-phase cubic fluorite materials. The lattice constants of the samples determined by whole-pattern Rietveld refinement are listed in Table 1. They increase linearly with increasing c_d (Vegard's law)[11] and are consistent with the ionic radii of Ce^{4+} (0.97 Å), Nd^{3+} (1.109 Å), and Sm^{3+} (1.079 Å).[12] A possible reduction in the oxidation state of cerium to Ce^{3+} during synthesis or consolidation would result in a positive deviation from the linear behavior because of the substantial difference in ionic radius between Ce^{3+} (1.143 Å)[12] and Ce^{4+} (0.97 Å), leading to lattice distortions.[13] The absence of such a behavior and the very light yellow color of all samples confirm that cerium in the NDC, SDC, and SNDC samples is fully oxidized to Ce^{4+}, which is in good agreement with previous studies.[14] All of the ceria solid solutions used for both calorimetry and impedance spectroscopy measurements were shown to be chemically homogenous by electron microprobe analysis, and no additional impurity phases were detected by backscattered electron images and X-ray dot maps, which is consistent with the XRD results. The compositions of the solid solutions determined by microprobe analysis agree well with the nominal compositions as shown in Table 1.

Figure 1 shows the Arrhenius plots of σ_i of NDC, SDC, and SNDC with different c_d. The densities of the pellets of $Ce_{1-x}Ln_xO_{2-0.5x}$ (Ln = Nd, Sm and $x = 0.05$, 0.10, 0.15, 0.20, and 0.25) used for the impedance measurements were above 94 % of the theoretical densities (see Table 2 for details). As O^{2-} conduction in ceria is a thermally activated process, σ_i increases exponentially with temperature according to the relation:

$$\sigma_i = \frac{\sigma_i^0}{T}\exp\left(-\frac{E_a}{k_B T}\right) \quad (1)$$

where T, σ_i^0, and k_B are the absolute temperature, the pre-exponential factor, and the Boltzmann constant, respectively. In general, E_a is considered to be the sum of the enthalpy of migration for V_O^{2+}, ΔH_m, and that of defect association (ΔH_a). The former represents the energy required for long-range hopping of V_O^{2+} randomly distributed in the PEL of "undoped" ceria (ca. 0.6 eV),[15] and the latter concerns the extra energy needed to dissociate V_O^{2+} from the defect associates, which may also include modulation of the PEL through elastic deformation of the lattice. The E_a values determined from the slopes of the Arrhenius plots for NDC, SDC, and SNDC over relatively low (150–400 °C) and high (400–650 °C) temperature ranges are listed in Table 2. The E_a values for lightly doped (< 10 mol %) samples are very close to the ΔH_m value of about 0.6 eV (58 kJ mol^{-1}), suggesting that the vast majority of the V_O^{2+} sites in these solid solutions are randomly distributed and freely mobile in the temperature range of interest. This is to be expected as any defect associates must dissociate as an infinite dilution is approached. Upon further doping (> 10 mol %), E_a increases rapidly with c_d (see Table 2), indicating the existence of defect associates at higher c_d, which trap V_O^{2+} even at relatively high temperatures. It should be noted that in heavily doped ceria, E_a is always higher than ΔH_m even at very high temper-

Table 1: Results of electron microprobe analyses, enthalpy of formation ($\Delta H_{f,ox}$) at 25 °C, enthalpy of formation ($\Delta H_{f,ox}$) at 702 °C, heat content ($\Delta_{25\,^\circ C}^{702\,^\circ C}H$) from transposed temperature drop calorimetry between 25 and 702 °C, lattice parameters, for the *x*SDC and *x*NDC cubic fluorite solid solutions and the end-members CeO_2, $SmO_{1.5}$, and $NdO_{1.5}$.

Sample	Actual composition[a] (*x*)	$\Delta H_{f,ox}$[10] (25 °C) [kJ mol^{-1}]	$\Delta H_{f,ox}$ (702 °C) [kJ mol^{-1}]	$\Delta_{25\,^\circ C}^{702\,^\circ C}H$ [kJ mol^{-1}][b]	Lattice parameters[c] [Å]
CeO_2	0			47.98 ± 0.07	
$SmO_{1.5}$	1			42.66 ± 0.32	
$NdO_{1.5}$	1			43.84 ± 0.24	
5SDC	0.048 ± 0.001	9.07 ± 1.17	8.01 ± 1.22	46.66 ± 0.34	5.4171 ± 0.0002
10SDC	0.092 ± 0.002	5.76 ± 1.30	8.63 ± 1.38	50.36 ± 0.45	5.4225 ± 0.0003
15SDC	0.152 ± 0.003	4.83 ± 1.05	7.69 ± 1.11	50.03 ± 0.35	5.4288 ± 0.0008
20SDC	0.191 ± 0.001	6.18 ± 1.02	6.80 ± 1.09	47.58 ± 0.37	5.4316 ± 0.0002
25SDC	0.245 ± 0.003	5.36 ± 1.19	6.30 ± 1.21	47.62 ± 0.20	5.4389 ± 0.0005
30SDC	0.294 ± 0.003	5.22 ± 1.16	6.08 ± 1.17	47.28 ± 0.09	5.4437 ± 0.0006
5NDC	0.046 ± 0.001	8.95 ± 1.30	8.07 ± 1.40	46.91 ± 0.52	5.4210 ± 0.0003
10NDC	0.097 ± 0.002	7.62 ± 1.74	8.79 ± 1.76	48.75 ± 0.27	5.4304 ± 0.0002
15NDC	0.132 ± 0.003	6.29 ± 1.12	8.09 ± 1.25	49.24 ± 0.55	5.4377 ± 0.0004
20NDC	0.189 ± 0.001	4.83 ± 1.08	7.15 ± 1.10	49.52 ± 0.22	5.4474 ± 0.0002
25NDC	0.240 ± 0.003	5.03 ± 1.14	6.34 ± 1.15	48.30 ± 0.14	5.4558 ± 0.0003
30NDC	0.302 ± 0.003	4.73 ± 1.26	5.29 ± 1.27	47.29 ± 0.11	5.4665 ± 0.0002
5SNDC	0.052 ± 0.001	4.29 ± 1.38	3.175 ± 1.38	46.61 ± 0.08	5.41847 ± 0.0001
10SNDC	0.101 ± 0.001	6.13 ± 1.06	5.08 ± 1.07	46.46 ± 0.11	5.42599 ± 0.0003
15SNDC	0.153 ± 0.004	4.30 ± 0.98	5.84 ± 0.99	48.79 ± 0.15	5.43320 ± 0.0002
20SNDC	0.201 ± 0.001	3.21 ± 1.27	6.09 ± 1.29	49.91 ± 0.23	5.44057 ± 0.0006
25SNDC	0.251 ± 0.001	4.12 ± 1.25	5.39 ± 1.26	48.06 ± 0.09	5.44781 ± 0.0003
30SNDC	0.297 ± 0.002	3.26 ± 0.87	3.89 ± 0.91	47.20 ± 0.25	5.45376 ± 0.0002

[a] Measured by wavelength dispersive spectroscopy (WDS). [b] $\Delta_{25\,^\circ C}^{702\,^\circ C}H = \int_{298\,K}^{975\,K} C_{p,m}dT$. Uncertainty: two standard deviations of the mean. [c] Lattice parameters of the solid solutions are determined by powder XRD least-squares analysis.

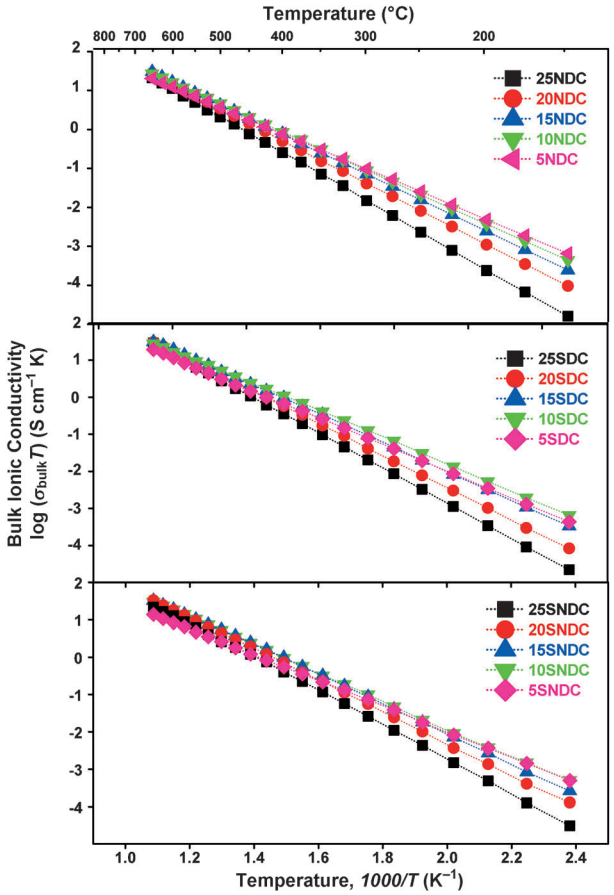

Figure 1. Arrhenius plot for the bulk ionic conductivities of $Ce_{1-x}Nd_xO_{2-0.5x}$ (NDC), $Ce_{1-x}Sm_xO_{2-0.5x}$ (SDC), and $Ce_{1-x}Sm_{0.5x}Nd_{0.5x}O_{2-0.5x}$ (SNDC; $0.05 \le x \le 0.25$).

atures as complete dissociation of V_O^{2+} may never occur before melting [e.g., ΔH_a of 25NDC is ca. 0.3 eV (30 kJ mol^{-1}) as shown in Table 2, which is equal to the thermal energy, k_BT, at ca. 3200 °C].

Figure 2 presents the $\Delta H_{f,ox}^{702\,^\circ C}$ determined for NDC, SDC, and SNDC from their constituent binary oxides at different c_d (for details, see the Supporting Information). The $\Delta H_{f,ox}^{702\,^\circ C}$ values are slightly endothermic regardless of c_d. Upon initial increase in c_d, $\Delta H_{f,ox}^{702\,^\circ C}$ becomes more endothermic to reach a maximum at approximately $x = 0.10$, 0.10, and 0.20 for NDC, SDC, and SNDC, respectively, and then becomes less endothermic with a further increase in c_d. As previously reported,[7] in dilute ceria solid solutions, the endothermic $\Delta H_{f,ox}$ is largely attributed to the lattice strain energy arising from vacancy formation as well as the mismatch between host and dopant cation size. At higher c_d, $\Delta H_{f,ox}$ of the solid solutions becomes increasingly less endothermic owing to the formation of various types of defect associates.[5,16] The contribution of defect association to $\Delta H_{f,ox}$ must be exothermic as the association results in a negative change in configurational entropy. Figure 2 also includes the bulk ionic resistivity, ρ_i ($=1/\sigma_i$), of NDC, SDC, and SNDC measured at 650 °C. (The resistance of the samples above this temperature is too small for accurate measurements within instrumental capabilities.) The ρ_i of all solid solutions shows a minimum (maximum conductivity) with increasing c_d, which is consistent with previous results for similar RE-doped ceria solid solutions.[2a,17] The minimum ionic resistivity, $\rho_{i,min}$ (i.e., $\sigma_{i,max}$), at 650 °C appears at $x = 0.15$ for NDC and SDC and at $x = 0.20$ for SNDC and gradually moves to lower c_d values with decreasing temperature (e.g., at 150 °C, $\rho_{i,min}$ appears at $x = 0.05$, 0.10, and 0.20 for NDC, SDC, and SNDC, respectively). Apparently, the c_d corresponding to the maximum $\Delta H_{f,ox}^{702\,^\circ C}$ reasonably coincides with c_d* (c_d yields $\rho_{i,min}$) at 650 °C. It is thus evident that the strong correlation between σ_i and $\Delta H_{f,ox}$ previously reported for RE-doped ceria near room temperature is maintained at the higher temperatures where IT-SOFCs are operated.

This correlation also manifests itself in Figure 3 in which the enthalpies of defect association at 702 °C ($\Delta H_a^{702\,^\circ C}$) calculated from the calorimetric data and the effective ΔH_a determined from impedance measurements at 400–650 °C are directly compared. The $\Delta H_a^{702\,^\circ C}$ was estimated from the difference between the enthalpy of mixing at 702 °C, $\Delta H_{mix}^{702\,^\circ C}$, and the corresponding curves from the regular solution model (i.e., $\Delta H_{mix}^{702\,^\circ C} = \Omega_{702\,^\circ C} x \cdot (1-x)$ for low dopant concentrations ($x < 0.10$), where $\Omega_{702\,^\circ C}$ is the interaction parameter). These calculations are analogous to those done for room temperature in our prior paper[7] (for details, see the

Table 2: Relative densities, activation energies (E_a) between 150 and 400 °C and 400 and 650 °C from impedance analyses, association enthalpy (ΔH_a) at 702 °C from calorimetric analyses, and association enthalpy (ΔH_a) between 400 and 650 °C from impedance analyses for *x*SDC, *x*NDC, and *x*SNDC.

Sample	Relative density[a] [%]	E_a ($T < 400\,^\circ C$) [kJ mol^{-1}]	E_a ($T > 400\,^\circ C$) [kJ mol^{-1}]	ΔH_a (702 °C) [kJ mol^{-1}]	ΔH_a (400–650 °C) [kJ mol^{-1}]
5SDC	97.0 ± 0.1	64.36 ± 0.29	63.97 ± 0.68	−0.04 ± 1.23	5.11 ± 0.68
10SDC	96.5 ± 0.1	65.42 ± 0.29	59.92 ± 0.48	−6.22 ± 2.25	1.06 ± 0.48
15SDC	96.5 ± 0.4	70.34 ± 0.19	65.90 ± 0.58	−15.38 ± 3.45	7.04 ± 0.58
20SDC	94.4 ± 0.1	78.54 ± 0.19	75.55 ± 0.39	−21.09 ± 4.14	16.69 ± 0.39
25SDC	94.3 ± 0.2	86.45 ± 0.19	84.62 ± 0.58	−27.45 ± 4.95	25.76 ± 0.58
30SDC				−32.27 ± 5.55	
5NDC	95.6 ± 0.1	62.04 ± 0.19	60.59 ± 0.48	−0.13 ± 1.43	1.83 ± 0.48
10NDC	96.9 ± 0.1	66.96 ± 0.19	64.07 ± 0.29	−7.46 ± 2.80	5.31 ± 0.29
15NDC	97.8 ± 0.1	70.92 ± 0.19	68.12 ± 0.39	−13.29 ± 3.67	9.26 ± 0.39
20NDC	99.6 ± 0.2	75.84 ± 0.29	74.87 ± 0.39	−21.72 ± 4.91	16.02 ± 0.39
25NDC	99.7 ± 0.2	86.93 ± 0.39	83.94 ± 0.58	−28.29 ± 5.83	25.09 ± 0.58
30NDC				−35.27 ± 6.73	
5SNDC	94.3 ± 0.2	60.50 ± 0.68	60.01 ± 0.68	0.00 ± 1.38	2.12 ± 0.68
10SNDC	96.6 ± 0.2	66.57 ± 0.96	64.45 ± 1.25	−0.71 ± 2.48	6.56 ± 1.25
15SNDC	98.9 ± 0.2	72.85 ± 0.39	64.36 ± 0.77	−2.74 ± 3.58	6.46 ± 0.77
20SNDC	97.6 ± 0.2	77.09 ± 0.87	71.50 ± 0.68	−4.82 ± 4.44	13.60 ± 0.68
25SNDC	97.7 ± 0.2	84.52 ± 0.68	74.97 ± 1.74	−7.74 ± 5.19	17.08 ± 1.74
30SNDC				−11.15 ± 5.77	

[a] Uncertainty: two standard deviations of the mean.

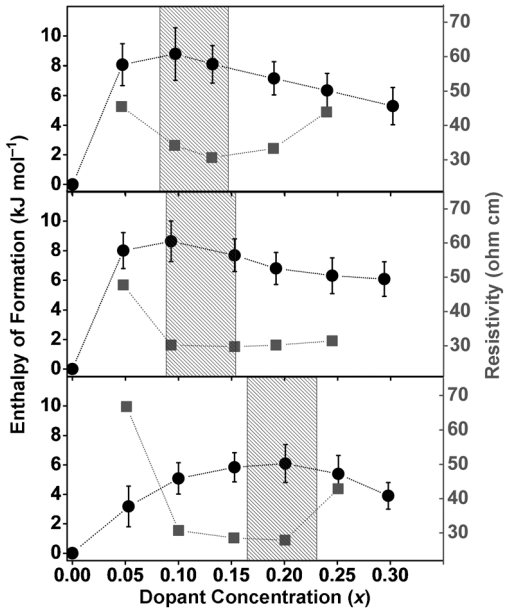

Figure 2. Enthalpies of formation at 702 °C (●) from end members of CeO_2, $SmO_{1.5}$, and $NdO_{1.5}$ and ionic resistivity at 650 °C (■) of NDC (top), SDC (middle), and SNDC (bottom) with respect to dopant concentration. Shaded areas represent the maximum and minimum value regions of the enthalpy of formation and the resistivity, respectively. Dotted lines connecting data points are visual aids.

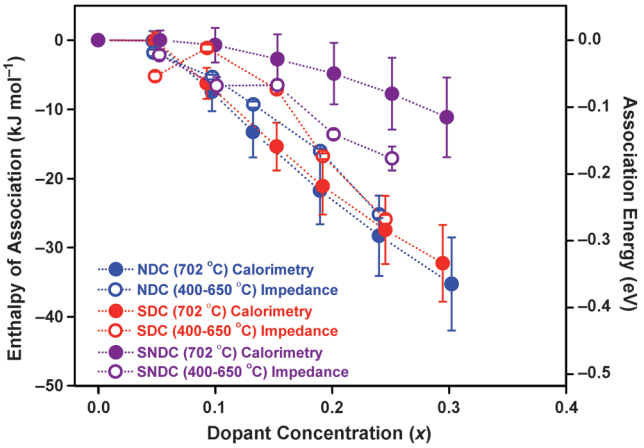

Figure 3. Enthalpies of defect association for NDC, SDC, and SNDC at 702 °C (●) from calorimetric analyses and the corresponding association energies between 400 and 650 °C (○) from impedance analyses as a function of dopant concentration. Dotted lines connecting data points are only a visual guide.

Supporting Information). The negative (stabilizing) deviation from the regular solution behavior at higher c_d is due to the formation of the defect associates. The effective ΔH_a is taken as the difference between E_a and ΔH_m of 0.6 eV (ca. 58 kJ mol^{-1}). The values of both association enthalpies and their dependence on c_d for the singly doped ceria solid solutions are in excellent agreement, especially considering that these parameters were determined independently. This is also true for the doubly-doped sample although the ΔH_a values are somewhat higher than the corresponding $\Delta H_a^{702\,^\circ C}$ values at $x = 0.20$ and above. Nonetheless, these results unambiguously confirm that σ_i and $\Delta H_{f,ox}^{702\,^\circ C}$ are strongly correlated with one another at higher temperatures.

It is worth noting that the energetics of formation of the doubly doped ceria differ from those of the singly doped counterparts, both at room temperature and at 702 °C. Upon an increase in temperature from 25 to 702 °C, the maximum $\Delta H_{f,ox}$ value for SNDC shifts from $x = 0.10$ to $x = 0.20$, whereas the shift occurs from $x = 0.05$ to $x = 0.10$ with a slight destabilization in maximum $\Delta H_{f,ox}$ for both NDC and SDC. The shift in the greatest energetic destabilization to higher c_d in SNDC compared to that of NDC and SNDC implies a greater dissociation of defect associates with increasing temperature in the doubly doped system, which is consistent with the less exothermic enthalpy of association seen at both ambient and high temperature.

To understand the energetics of dissociation, the $\Delta_{25\,^\circ C}^{702\,^\circ C} H_{xs}$ values (Figure 4) were also calculated for both singly and doubly doped systems. $\Delta_{25\,^\circ C}^{702\,^\circ C} H_{xs}$ is the deviation of the heat content of a solid solution from the stoichiometric sum of the

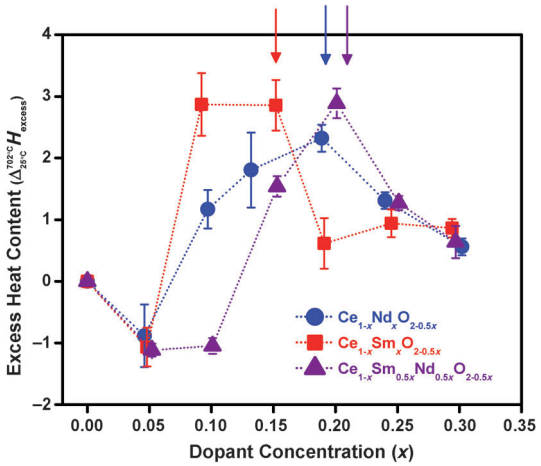

Figure 4. Excess heat contents of NDC, SDC, and SNDC ($0.05 \le x \le 0.30$) from room temperature to 702 °C. $\Delta_{25\,^\circ C}^{702\,^\circ C} H_{xs}$ with respect to dopant concentration. The arrows mark the critical dopant concentrations that yield the maximum defect disordering near 700 °C for a given solid solution.

heat contents of its binary oxides between room temperature and 702 °C. The most positive $\Delta_{25\,^\circ C}^{702\,^\circ C} H_{xs}$ occurs in the same c_d range where the pronounced shift in c_d* occurs. This indicates that defect clusters dissociate to some extent between room temperature and 702 °C. As defect dissociation is thermally activated, it is energetically unfavorable, yet entropically favorable; consequently the degree of associate formation diminishes with increasing temperature, with the most positive $\Delta_{25\,^\circ C}^{702\,^\circ C} H_{xs}$ at $x = 0.15$ to 0.20. Furthermore, $\Delta_{25\,^\circ C}^{702\,^\circ C} H_{xs}$ diminishes to very slightly endothermic values at high c_d values, which further supports significant dissociation of defect associates at intermediate c_d ($0.10 < x < 0.20$).

For the first time, the correlations between energetics and σ_i of singly and doubly doped ceria with neodymia and

samaria at high temperatures have been confirmed using a combination of transposed temperature drop calorimetry and impedance spectroscopy. The maximum $\Delta H_{f,ox}$ values coincide with $\sigma_{i,max}$ at molar dopant fractions of 0.10, 0.15, and 0.20 in $Ce_{1-x}Nd_xO_{2-0.5x}$, $Ce_{1-x}Sm_xO_{2-0.5x}$, and $Ce_{1-x}Sm_{0.5x}Nd_{0.5x}O_{2-0.5x}$, respectively. This result demonstrates that calorimetric studies can provide a definitive understanding of the energetics of SOFC electrolytes and assist in tailoring such electrolytes to achieve optimum $\sigma_{i,max}$ values.

Received: April 23, 2014
Published online: July 9, 2014

Keywords: ceria · doping · ionic conductivity · materials science · solid solutions

[1] B. C. H. Steele, *J. Power Sources* **1994**, *49*, 1 – 14; J. B. Goodenough, *Annu. Rev. Mater. Res.* **2003**, *33*, 91 – 128.
[2] H. Inaba, H. Tagawa, *Solid State Ionics* **1996**, *83*, 1 – 16; L. Malavasi, C. A. J. Fisher, M. S. Islam, *Chem. Soc. Rev.* **2010**, *39*, 4370 – 4387.
[3] A. A. Yaroshevsky, *Geochem. Int.* **2006**, *44*, 48 – 55; K. H. Wedepohl, *Geochim. Cosmochim. Acta* **1995**, *59*, 1217 – 1232.
[4] S. Sen, T. Edwards, S. K. Kim, S. Kim, *Chem. Mater.* **2014**, *26*, 1918 – 1924.
[5] M. Nakayama, M. Martin, *Phys. Chem. Chem. Phys.* **2009**, *11*, 3241 – 3249; M. Burbano, S. T. Norberg, S. Hull, S. G. Eriksson, D. Marrocchelli, P. A. Madden, G. W. Watson, *Chem. Mater.* **2011**, *23*, 222 – 229.
[6] A. Navrotsky, *J. Mater. Chem.* **2010**, *20*, 10577 – 10587.
[7] W. Chen, A. Navrotsky, *J. Mater. Res.* **2006**, *21*, 3242 – 3251.
[8] H. J. Avila-Paredes, T. Shvareva, W. Chen, A. Navrotsky, S. Kim, *Phys. Chem. Chem. Phys.* **2009**, *11*, 8580 – 8585.
[9] M. Aizenshtein, T. Y. Shvareva, A. Navrotsky, *J. Am. Ceram. Soc.* **2010**, *93*, 4142 – 4147.
[10] S. Buyukkilic, T. Shvareva, A. Navrotsky, *Solid State Ionics* **2012**, *227*, 17 – 22.
[11] L. Vegard, *Z. Phys.* **1921**, *5*, 17 – 26.
[12] R. Shannon, *Acta Crystallogr. Sect. A* **1976**, *32*, 751 – 767.
[13] S. Hull, S. T. Norberg, I. Ahmed, S. G. Eriksson, D. Marrocchelli, P. A. Madden, *J. Solid State Chem.* **2009**, *182*, 2815 – 2821.
[14] L. Li, J. C. Nino, *J. Eur. Ceram. Soc.* **2012**, *32*, 3543 – 3550; L. Aneflous, J. A. Musso, S. Villain, J.-R. Gavarri, H. Benyaich, *J. Solid State Chem.* **2004**, *177*, 856 – 865; S. Omar, E. D. Wachsman, J. L. Jones, J. C. Nino, *J. Am. Ceram. Soc.* **2009**, *92*, 2674 – 2681.
[15] D. Y. Wang, D. S. Park, J. Griffith, A. S. Nowick, *Solid State Ionics* **1981**, *2*, 95 – 105.
[16] D. A. Andersson, S. I. Simak, N. V. Skorodumova, I. A. Abrikosov, B. Johansson, *Proc. Natl. Acad. Sci. USA* **2006**, *103*, 3518 – 3521.
[17] S. Omar, E. D. Wachsman, J. C. Nino, *Solid State Ionics* **2008**, *178*, 1890 – 1897; I. E. L. Stephens, J. A. Kilner, *Solid State Ionics* **2006**, *177*, 669 – 676; G. B. Balazs, R. S. Glass, *Solid State Ionics* **1995**, *76*, 155 – 162; L. Li, R. Kasse, S. Phadke, W. Qiu, A. Huq, J. C. Nino, *Solid State Ionics* **2012**, *221*, 15 – 21.

